IEICE Proceeding Series

A Similarity on Energy Exchange Between Resonance and Synchronization

Madoka Kubota, Takashi Hikihara

Vol. 1 pp. 926-929
Publication Date: 2014/03/17
Online ISSN: 2188-5079

2012 International Symposium on Nonlinear Theory and its Applications
NOLTA2012, Palma, Majorca, Spain, October 22-26, 2012

A Similarity on Energy Exchange Between Resonance and Synchronization

Madoka Kubota† and Takashi Hikihara‡

†‡Department of Electrical Engineering, Kyoto University
Katsura, Nishikyo, Kyoto, 615-8510 Japan
Email: †kubota@dove.kuee.kyoto-u.ac.jp, ‡hikihara@kuee.kyoto-u.ac.jp

Abstract—This research focuses on a possibility to scavenge energy from fluid flow including turbulence. Based on turbulent mechanics, energy scavenging devices are expected to have nonlinear characteristics to accept wide-band-spectrum power distributed in turbulence. A magnetoelastic beam is adopted as one of candidates of energy scavenging devices. The magnetoelastic beam is excited in a nonlinear magnetic field formed by two magnets. In this paper, we estimate the possibility of energy exchange at synchronization as the scavenging mechanism, with considering the similarity to resonance.

1. Introduction

Watermills and windmills utilize averaged fluid flows over a critical velocity. There is an idea to decompose the flow velocity into the average and the fluctuating components [1]. Such fluctuations included in turbulence have a potential to supply energy to collecting devices using a suitable mechanism. It is well known that the developed turbulence consists of vibration with widely spread power spectrum [2]. This is because spatial self similarities appear in the extremely developed turbulence [3, 4]. However it has not been found which mechanism is available to scavenge the power distributed over wide frequency range using a low DOF (degree of freedom) device. Several studies focused on energy collected by an oscillation at resonance [5, 6]. Here, a clue to collect energy from turbulence exists in the application of nonlinear devices based on turbulent dynamics. In this paper, a chaotic oscillation, generated by a magnetoelastic beam [7], is adopted as an energy source which has broad power spectrum similar to turbulence. For the simplicity of experiment, a magnetoelastic beam is also selected as a scavenging device. As mentioned above, a chaotic oscillation has a broad power spectrum as energy source. When a single frequency is collected at resonance, the rest of power is discarded. On the other hand, the chaotic synchronization [8, 9] is possible to transfer the energy between systems within distributed frequency range. In this paper, our interest is in an energy exchange characteristic at synchronization. This characteristic leads the conjecture that one of the keys for energy scavenging from turbulence is a synchronization mechanism. In Sec.2, the possibility of energy exchange at resonance are confirmed. In Sec.3, a system which attains synchronization between two magnetoelastic beam subsystems is introduced. In Sec.4, the analysis of energy exchange is carried out at synchronization and similarities to resonance are discussed. Sec.5 concludes this paper.

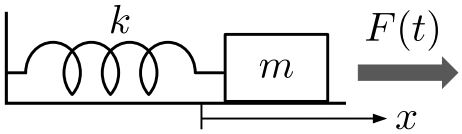

Figure 1: A forced spring-mass system.

2. Energy exchange at resonance

In this section, the energy exchange is described using a spring-mass system with an external force. Fig.1 shows the system excited by an external force $F(t)$ and subjected to friction. The relationship is governed by the following equation:

$$m\ddot{x} + kx + \Gamma\dot{x} = F(t), \tag{1}$$

where m denotes the mass, k the spring constant, and Γ the damping constant. ($\dot{}$) represents $\mathrm{d}/\mathrm{d}t$. Eq.(1) can be divided by m as

$$\ddot{x} + \gamma\dot{x} + {\omega_0}^2 x = f_0 \cos\omega t, \tag{2}$$

where $\omega_0 = k/m$, $\gamma = \Gamma/m$, and $f_0 \cos\omega t = F(t)/m$. The solution is obtained as

$$x = A\cos\omega t + B\sin\omega t, \tag{3}$$

where A and B are given as follows

$$A = \frac{f_0({\omega_0}^2 - \omega^2)}{({\omega_0}^2 - \omega^2)^2 + \gamma^2\omega^2}, \tag{4}$$

$$B = \frac{f_0\gamma\omega}{({\omega_0}^2 - \omega^2)^2 + \gamma^2\omega^2}. \tag{5}$$

Fig.2 shows the amplitude response curves to the external force frequency ω at the parameters $f_0 = 1.0, \omega_0 = 4.0$, and $\gamma = 0.1$. In this system, ω_0 is a natural frequency of undamped oscillation.

When the external force $F(t)$ works to the mass, the work gives power $P(t)$ per a unit of time. $P(t)$ is defined by "force $\times$ velocity" as

$$P(t) = mf_0 \cos\omega t(-A\omega\sin\omega t + B\omega\cos\omega t). \tag{6}$$

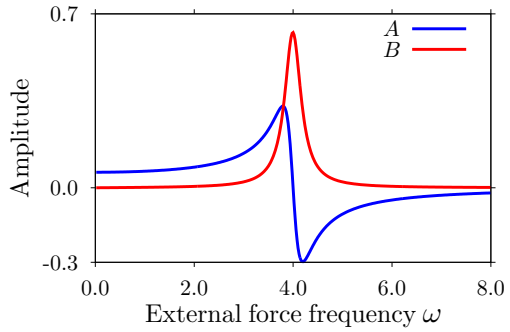

Figure 2: Amplitude response curves for the external force frequency. The figure shows the change in amplitude A (red line) and B (blue line) of Eq.(3) at $f_0 = 1.0, \omega_0 = 4.0$, and $\gamma = 0.1$.

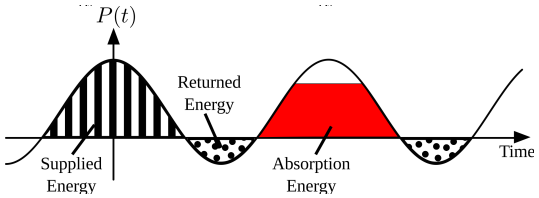

Figure 3: Schematic diagram of power oscillation. It explains supplied, returned, and absorption energy.

Fig.3 shows a schematic diagram of power $P(t)$. The vertically striped area indicates supplied energy from $F(t)$, and the dotted area does the returned energy from $F(t)$. The returned energy implies that the mass-spring system returns energy back to the external force. The red colored part represents the absorbed energy equals to the balance between supplied energy and returned energy. It also equals to dissipation energy: $\int \gamma \dot{x}^2 dt$. Fig.4 shows the frequency dependencies of supplied energy (green line), returned energy (blue line), and absorption energy (red line) during one period $2\pi/\omega$. The frequency ω was swept from 0.0 to 8.0. Fig.4 exhibits the absorption energy takes the maximum value and the returned energy minimum at resonance. Comparing Figs.2 and 4, the absorption energy is related to the amplitude B, and the returned one to the amplitude A. Fig.5 shows the frequency dependencies of the absorption (red line) and returned (blue line) energy rates to the supplied energy. The frequency of the external force determines whether the mass absorbs or returns the supplied energy. It can be clearly found that the absorption energy rates become 1.0 and the returned energy rate shows 0.0 at the resonant frequency. In the next section, we extend the considerations to the analysis of synchronization.

3. Synchronized systems

To prepare the consideration of energy exchange at synchronization, a coupled system is introduced. Volos et al. confirmed a period-1 synchronization between two Duffing subsystems using two-way signals [10]. According

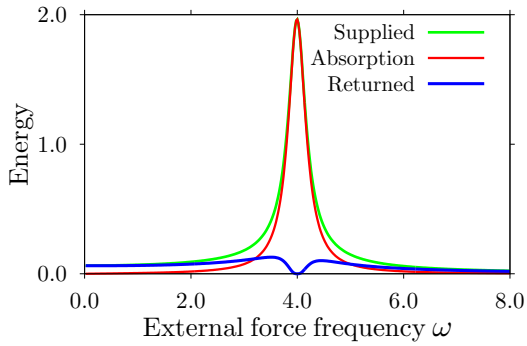

Figure 4: Energy response curves for the external force frequency. The figure shows the change in supplied energy (green line), returned energy (blue line) and absorption energy (red line).

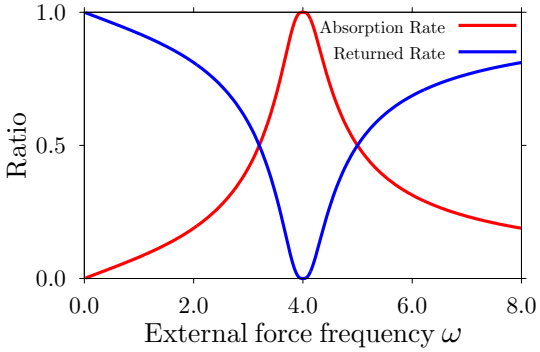

Figure 5: Energy rates response curves for the external force frequency. The figure shows the change in absorption (red line) and returned (blue line) energy rates to supplied energy.

to their results, we proposed another system consisting of three Duffing subsystems as in Fig.6. The system shows synchronization within wide frequency range. The whole system is described as

$$\text{Exciter} : \ddot{u}_0 + \gamma \dot{u}_0 + \frac{1}{2}({u_0}^2 - 1)u_0 = b \cos \omega_0 t, \quad (7)$$

$$\text{Subsystem 1} : \ddot{u}_1 + \gamma \dot{u}_1 + (1-\xi)\frac{1}{2}({u_1}^2 - 1)u_1 + \xi \frac{1}{2}({u_2}^2 - 1)u_2 = K u_0, \quad (8)$$

$$\text{Subsystem 2} : \ddot{u}_2 + \gamma \dot{u}_2 + (1-\xi)\frac{1}{2}({u_2}^2 - 1)u_2 + \xi \frac{1}{2}({u_1}^2 - 1)u_1 = K u_0, \quad (9)$$

where u_0 denotes the displacement of the exciter. In addition, u_1 and u_2 denote the displacements of the subsystems 1 and 2, respectively. γ denotes the damping constant, b the amplitude, and ω_0 the angular velocity of external force within the exciter. Eqs.(7), (8) and (9) are nondimensionalized. In the system, subsystems 1 and 2 can be synchronized. As shown in Eqs.(8) and (9), subsystems 1 and 2 are coupled at a coupling factor ξ, and exchange interactions

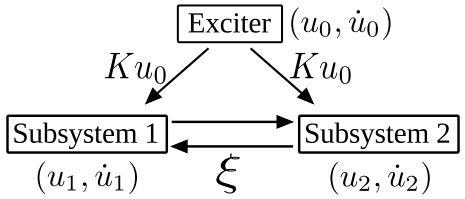

Figure 6: Composition of two Duffing subsystems and the exciter. This enables synchronization between subsystem 1 and subsystem 2.

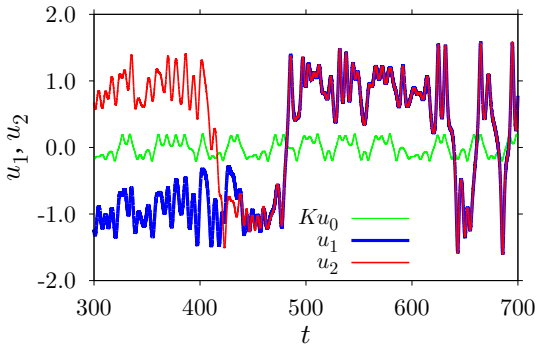

Figure 7: Displacements Ku_0, u_1, and u_2 at $\xi = 0.44$, $\gamma = 0.1, b = 0.12, K = 0.14$, and $\omega_0 = 0.74$

as coupling force. When the coupling factor $\xi \leq 0.13$, the coupled subsystems 1 and 2 are trapped in one of the potential wells, depending on the initial condition. To make it easier for subsystems 1 and 2 to bounce out from one potential well to the other, the exciter generates one-way oscillation force Ku_0 to subsystems 1 and 2. Fig.7 shows synchronization between u_1 and u_2 at $\xi = 0.44$. The synchronization appears after $t = 450$. Here, the synchronization depends on the coupling factor ξ increased from 0.40 to 0.50 as shown in Fig.8. In the figure, all dots represent time averaged $|u_1 - u_2|$ during $3000 \leq t \leq 12000$. From ξ=0.423 to ξ=0.473, the difference between u_1 and u_2 becomes almost 0. Therefore subsystems 1 and 2 synchronize to each other.

4. Energy exchange at synchronization

According to the features of energy exchange at resonance, we examine the synchronization. From Eq.(8), the total external force to subsystem 1 is amounted to $-\xi\frac{1}{2}({u_2}^2 - 1)u_2 + Ku_0$, consequently power $P(t)$ is obtained as

$$P(t) = \{-\xi\frac{1}{2}({u_2}^2 - 1)u_2 + Ku_0\}\dot{u}_1. \quad (10)$$

$P(t)$ is shown in Fig.9. The integration of positive $P(t)$ corresponds to the supplied energy, the integration of negative $P(t)$ to the returned energy, and the balance to the absorption energy which equals to dissipation energy: $\int \gamma \dot{u}_1^2 dt$. In Fig.10, the absorption energy and returned energy rates to

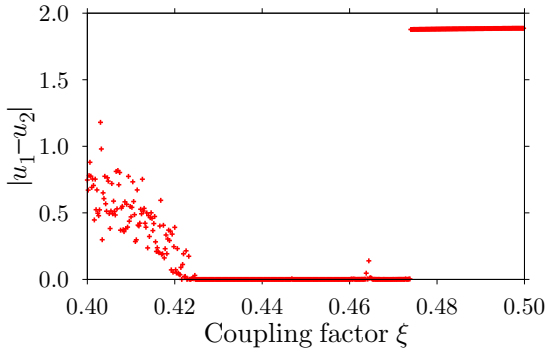

Figure 8: Synchronization detection by time averaged absolute values of the difference between u_1 and u_2 ($3000 \leq t \leq 12000$) versus the coupling factor ξ.

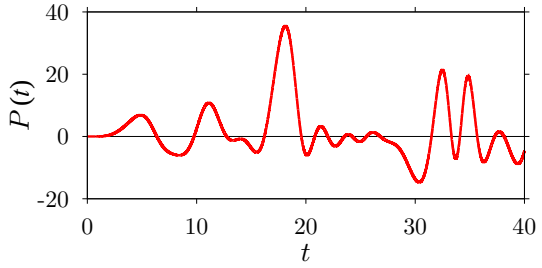

Figure 9: Power time series in Eq.(10) for ξ =0.44.

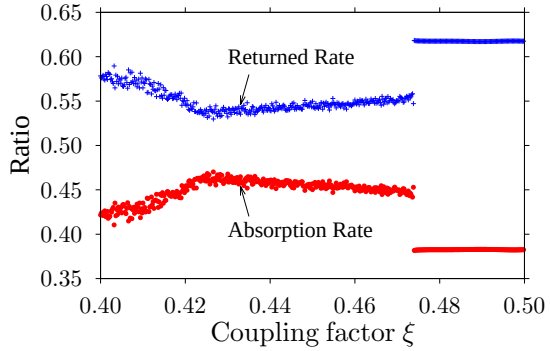

Figure 10: Dots show the change in absorption (•) and returned (+) energy rates to the supplied energy for the coupling factor ξ.

the supplied energy are represented depending on the coupling factor ξ. From Figs.8 and 10, the absorption energy rate maintains higher rate within synchronization around $\xi = 0.423$. The returned energy rate shows vice varsa. These tendencies show the similarity to the results obtained at resonance in Fig.5. In this figure, the frequency ω of the external force governs the energy rates. On the other hand in Fig.10, the coupling factor ξ governs the energy rates. Thereby ω and ξ seem to have a similarity. The change of ω around resonance directly implies the regulation of phase difference when the external force is fixed. This is because the phase difference is described as $\arctan(B/A)$, whose A and B can be regulated by ω. In power engineering, power factor shows the efficiency that the load draws the real power. In a theoretical view point, it is pos-

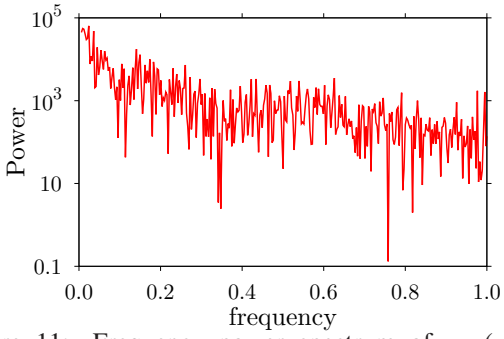

Figure 11: Frequency power spectrum of u_1 (=u_2) at ξ =0.44. Wide frequency range is observed.

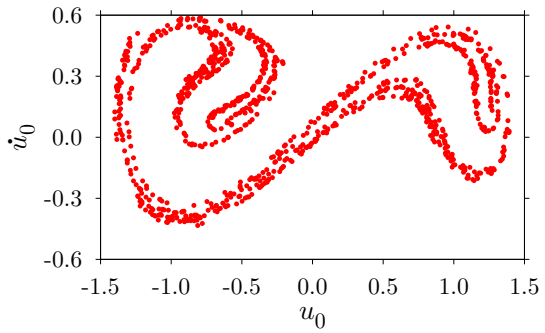

Figure 12: Numerical strobo map of the exciter on $(u_0, \dot{u}_0)$ at every $2\pi/\omega_0$ for ξ =0.44.

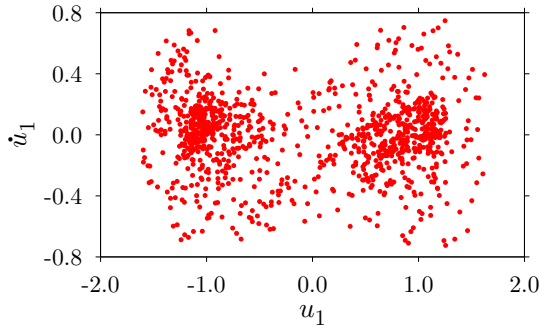

Figure 13: Numerical strobo map of subsystem 1 on $(u_1, \dot{u}_1)$ at every $2\pi/\omega_0$ for ξ =0.44. $(u_1, \dot{u}_1) = (u_2, \dot{u}_2)$ because of synchronization.

sible to discuss the relationship between the phase difference and the energy flow at synchronization of oscillation [11]. However as in Fig.11, the chaotic system exhibits widely distributed spectrum. Therefore at chaotic synchronization, phase difference at a single frequency cannot be used as a distance between two oscillators. Hence the new definition of the distance is requested for chaotic synchronization. The coupling factor ξ seems one of the distance parameters.

Fig.12 shows the stroboscopic map of the exciter on $(u_0, \dot{u}_0)$ at every $2\pi/\omega_0$, and Fig.13 also shows the stroboscopic map of subsystem 1 on $(u_1, \dot{u}_1)$. At synchronization $(u_1, \dot{u}_1) = (u_2, \dot{u}_2)$. As Fig.13, the subsystem 1 doesn't show a clear structure of strange attractor like Fig.12. This unclear structure is one of the features of higher dimensional chaos. However, the widely distributed spectrum, observed as in Fig.11, maintains the turbulent feature at the synchronization. This is the significant characteristic of the energy scavenging using nonlinear devices.

5. Conclusion

This paper discusses the energy scavenging from turbulence, in which power is widely distributed over the frequency range. Considering the spread spectrum feature, chaotic synchronization mechanism seemed to have a possibility to transfer the turbulent energy to mechanical or electrical energy. The significant result here is that energy exchange features were confirmed at synchronization between two subsystems. Synchronization is attained between two coupled Duffing subsystems by exchanging signals as force. Energy exchange showed the features that the dissipation energy rate to supplied energy increases at synchronization. This energy exchange feature at synchronization is similar to the feature obtained at resonance. This result is the first step to design scavenging devices from turbulence.

Acknowledgment

One of the authors (M. K.) thanks Dr. Yokoi, Nagasaki Univ, for the fruitful discussion about synchronization.

References

[1] H. Tennekes and J. L. Lumley, A First Course in Turbulence, The MIT Press, Chap.2, 1973.

[2] D. Ruelle and F. Takens, *Commun. math. Phys.*, vol. 20, no. 3, pp. 167–192, 1971.

[3] M. Tanahashi, T. Miyauchi, and J. Ikeda, IUTAM Symp.: Simulation and Identification of Organized Structures in Flows, pp. 131-140, 1999.

[4] Y. Wang, M. Tanahashi, and T. Miyauchi, *Int. J. Heat Fluid Flow*, vol. 28, pp. 1280-1290, 2007.

[5] M. M. Bernitsas, K. Raghavan, Y. Ben-Simon and E. M. H. Garcia, *J. Offshore Mech. Arctic Eng.*, vol. 132, no. 4, pp. 041101-1–041101-15, 2008.

[6] D. A. W. Barton, S. G. Burrow and L. R. Clare, *J. Vib. Acoust.*, vol. 132, no. 2, pp. 021009-1–021009-7, 2010.

[7] F. C. Moon and P. J. Holmes, *J. Sound Vib.*, vol. 65, no. 2, pp. 275–296, 1979.

[8] L. M. Pecora and T. L. Carroll, *Phys. Rev. Lett.*, vol. 64, no. 8, pp. 821–824, 1990.

[9] L. M. Pecora and T. L. Carroll, *Phys. Rev. A.*, vol. 44, no.48, pp. 2374–2383, 1991.

[10] C. K. Volos, I. M. Kyprianidis, and I. N. Stouboulos, *International Journal of circuits, Systems and Signal Processing*, Issue. 3, vol. 1, pp. 274–281, 2007.

[11] Y. Yokoi, PhD dissertation, Kyoto University, March 2010.